

Combustion Analysis by Two-Zone Model in a DI Diesel Engine

M.Ishida, Z.L.Chen, H.Ueki and D.Sakaguchi

*Nagasaki University
1-14 Bunkyo-machi, Nagasaki 852
Japan*

ABSTRACT

In the proposed two-zone model consisting of a burned zone and an unburned zone in the combustion chamber, the changing process is thermodynamically independent except that the air is entrained from the unburned zone to the burned zone in accordance with the specified excess air ratio pattern during combustion. The excess air ratio λ_d is assumed to be constant in the diffusion combustion duration. The calculated time histories of the burned zone gas temperature and the net soot formation agree quantitatively or qualitatively with the experimental ones measured by the infrared two-color method, except for the prediction of the swirl effect. It was also shown that λ_d is mainly dominated by the fuel spray characteristics and ignition delay through the steady diffusion flame model analysis. In addition, the major factor of NOx reduction was analyzed using this two-zone model mainly on the point of view of the excess air ratio.

INTRODUCTION

There are many kinds of combustion analysis model for diesel engines. The one-dimensional heat release analysis is the most simple and useful one, however, the one-dimensional homogeneous model is not suitable for analyzing formations of NOx and soot. Therefore, the one-dimensional heterogeneous model with the stochastic mixing process has been proposed by Ikegami et al.⁽¹⁾. Many two-zone models have been proposed by Aoyagi et al.⁽²⁾, by Hatakeyama⁽³⁾, by Morel et al.⁽⁴⁾ respectively in accordance with their research objectives. On the other hand, the multi-zone model has been proposed by Hiroyasu et al.⁽⁵⁾. In the present paper, the authors have proposed a new two-zone model in order to estimate the excess air ratio in the burned zone, where the excess air ratio λ_d was assumed to be constant in the diffusion combustion duration, and was determined through some iterative calculations so as to coincide the NOx concentrations between the experiment and the analysis, and the calculated net soot was also made to be identical with the measured smoke density. It is well known that the soot formation is strongly dependent on the local gas temperature and the local excess air ratio, however, the maximum burned gas temperature is the first-order factor for the NO formation, and the burned gas temperature in the latter half of the combustion period is for the

soot oxidization. Therefore, the big stress was put on the accurate estimation of the excess air ratio in the burned zone.

ANALYSIS MODEL

Two-Zone Model

The basic assumptions of the present two-zone model are as follows; (1) The in-cylinder gas region is divided into two zones, that is, a burned gas zone and an unburned gas zone. The gas in each zone is uniform and changes independently with the same pressure under the adiabatic condition. (2) The gas weight in the burned zone is the sum of the burned fuel and the entrained air, and an unburned fuel is included in the unburned zone with the induced suction air and the residual gas.

Figure 1 show some patterns of excess air ratio in relation to the heat release rate. As mentioned above, it is a distinguishing mark in the present model that the excess air ratio is assumed to be constant during the diffusion combustion period, and four kinds of pattern are assumed in the premixed combustion period. Comparing the analytical results with the experimental ones, the type P-2 was seemed to be the most appropriate one. The ignition occurs under the theoretical mixture condition, and it varies continuously from $\lambda_{po}=1.0$ at the ignition timing until the final mean excess air ratio λ_m at the exhaust valve opening timing.

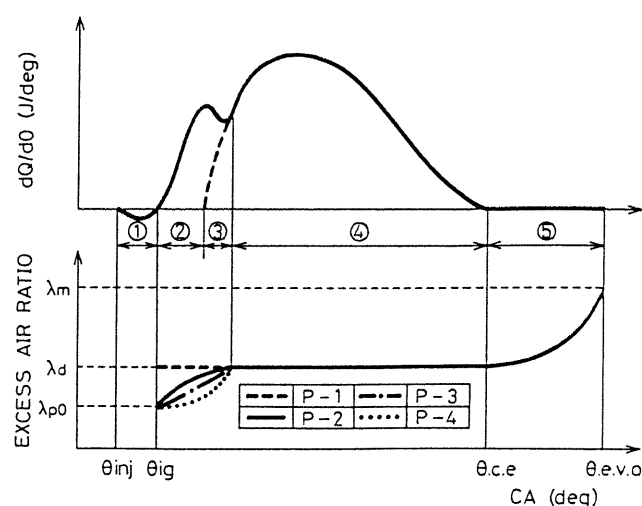


Fig.1 The assumed excess air ratio patterns in relation to heat release rate

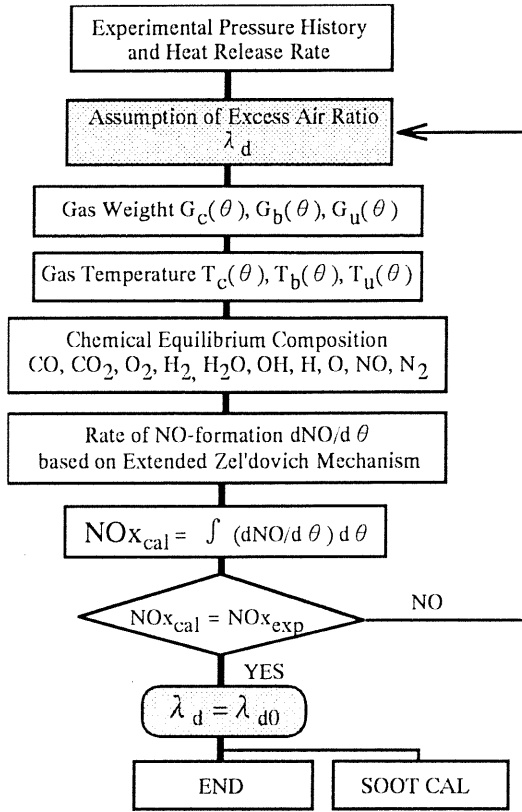


Fig.2 Flow-chart of calculation

Table 1 Equations used in the present two-zone model

Calculation of Gas Temperatures

Average gas temperature in the cylinder

$$T_c = PV / G_c R$$

Unburned-zone gas temperature

$$T_u = T_0 (P/P_0)^{(k-1)/k}$$

Burned-zone gas temperature

$$T_b = \{ G_c c_{vc} T_c - G_u c_{vu} T_u \} / G_b c_{vb}$$

Calculation of NO-formation Rate based on Extended Zel'dovich Mechanism

$$d[NO]/dt = a \{ k_1 [N_2][O] - b [NO]^2 \}$$

$$a = \{ 2(k_2[O_2] + k_3[OH]) \} / \{ r_1[NO] + k_2[O_2] + k_3[OH] \}$$

$$b = \{ r_1 r_2 [O] + r_1 r_3 [H] \} / \{ k_2 [O_2] + k_3 [OH] \}$$

Calculation of Soot-formation and -burnup by Morel's Model

$$(dS/dt)_f = A_1 m_d \exp[-A_2/T_b]$$

$$(dS/dt)_b = \{ B_1 S / \rho_s d_s \} \exp[-B_2/T_{rad}] \sqrt{P O_2}$$

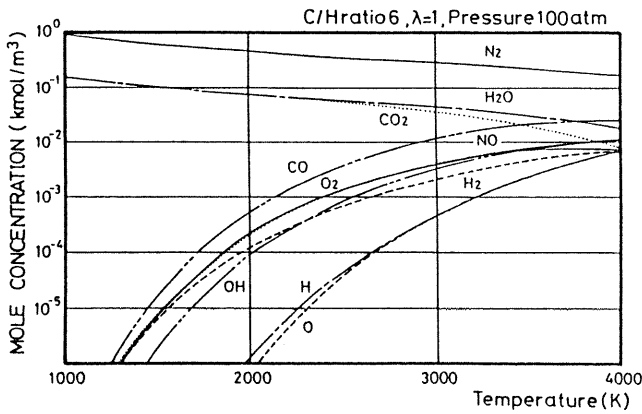
$$(dS/dt)_{net} = (dS/dt)_f - (dS/dt)_b$$

Calculation Procedure

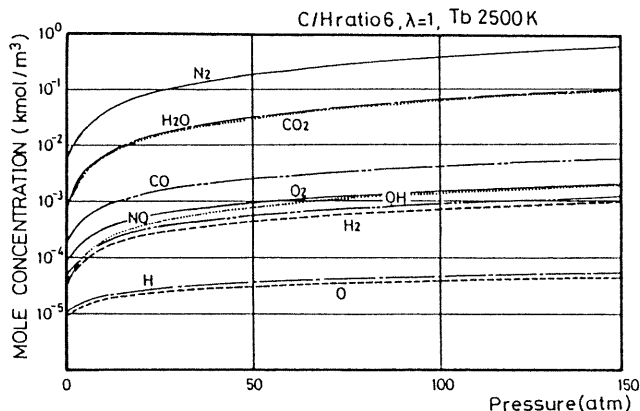
After assuming an initial value of λ_d , the calculation is proceeded in accordance with the flow-chart shown in Fig.2 under the given conditions of the experimental pressure history and the rate of heat release. The weight of the burned fuel G_f is estimated by the heat release rate based on the measured combustion pressure history, the gas weight in the burned zone is by $G_b = (1 + \lambda L_{th}) G_f$ and the unburned gas weight is by $G_u = G_c - G_b$; where L_{th} is the theoretical air quantity for the fuel and G_c is the total gas weight in the cylinder which includes the weight of injected fuel. Table 1 shows the equations used here for the calculations of the gas temperatures and the rates of NO formation, soot formation and soot oxidation.

NO formation rate is calculated by the equation based on the extended Zel'dovich mechanism where the ten kinds of chemical equilibrium compositions are taken into consideration except for NO. As shown in the above equation, NO formation rate is mainly dominated by the mole concentrations of [O] and [N₂]. Figures 3(a) and (b) show the variation of equilibrium mole concentrations due to temperature or pressure respectively in the ten chemical compositions. It is clear that the mole concentration of [O] is decreased significantly by lowering the temperature, and also the mole concentrations of both [N₂] and [O] are decreased by lowering the pressure.

The converged value λ_{d0} of the excess air ratio is determined through some iterative calculations if the calculated NOx concentration coincided with the measured one. As a result, the burned gas temperature is determined, and then the soot calculation follows; where the net soot formation rate is estimated so as to coincide the smoke densities between the experiment and the analysis by using the equations proposed by Morel et al.⁽⁴⁾



(a) Temperature variation



(b) Pressure variation

Fig.3 Chemical equilibrium composition

TEST ENGINE AND MEASUREMENT SYSTEM

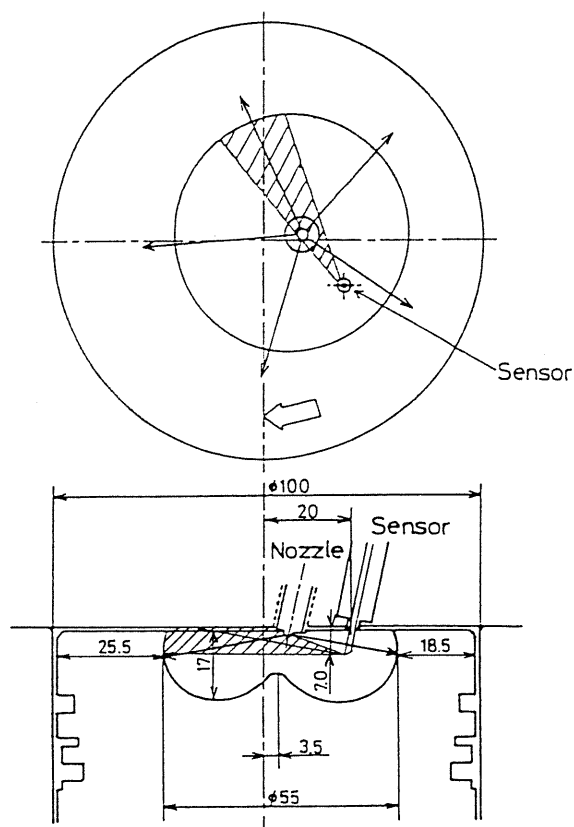


Fig.4 Combustion chamber configuration and measuring volume

Test engine was a four-cylindered high-speed turbocharged direct injection diesel engine with the intercooler system; which is the type 4D31-T manufactured by Mitsubishi Motor Corporation. It has a bore of 100 mm, a stroke of 105 mm and a maximum output of 95.6 kW(130 PS)/3,500 rpm. Test fuel was an automobile diesel oil named here ADO60 having a cetane index of about 60 and, in addition, low cetane fuels ADO45 and ADO40 were used in a part for comparison. For measuring the time histories of the flame temperature and the soot concentration, the beveled-edge type light pipe sensor was used, which is a 1.27 mm diameter smooth sapphire rod with the wedge-shaped leading edge cut by 45 degrees to the sensor rod axis. The sensor was inserted into the combustion chamber through the glow-plug hole of the engine and the flame temperature measuring volume was shown by the hatched region in Fig.4, in which also shown the combustion chamber configuration and the direction of five fuel spray axes by solid lines with arrow. The temperature measuring system consists of the light pipe sensor, the optical fiber thermometer (OFT) Model 100C manufactured by Accufiber Corp., the multi-channel combustion analyzer Model CB-466 by Ono Sokki Co. Ltd., and a personal computer. Two infrared wavelengths of 950 and 800 nm were selected in this system for the two-color method. The radiant energy of the two wavelengths detected by the OFT was transmitted to the combustion analyzer as a couple of voltage output, and it was collected and recorded on floppy disc as data for every 1/4 degree in crank angle.

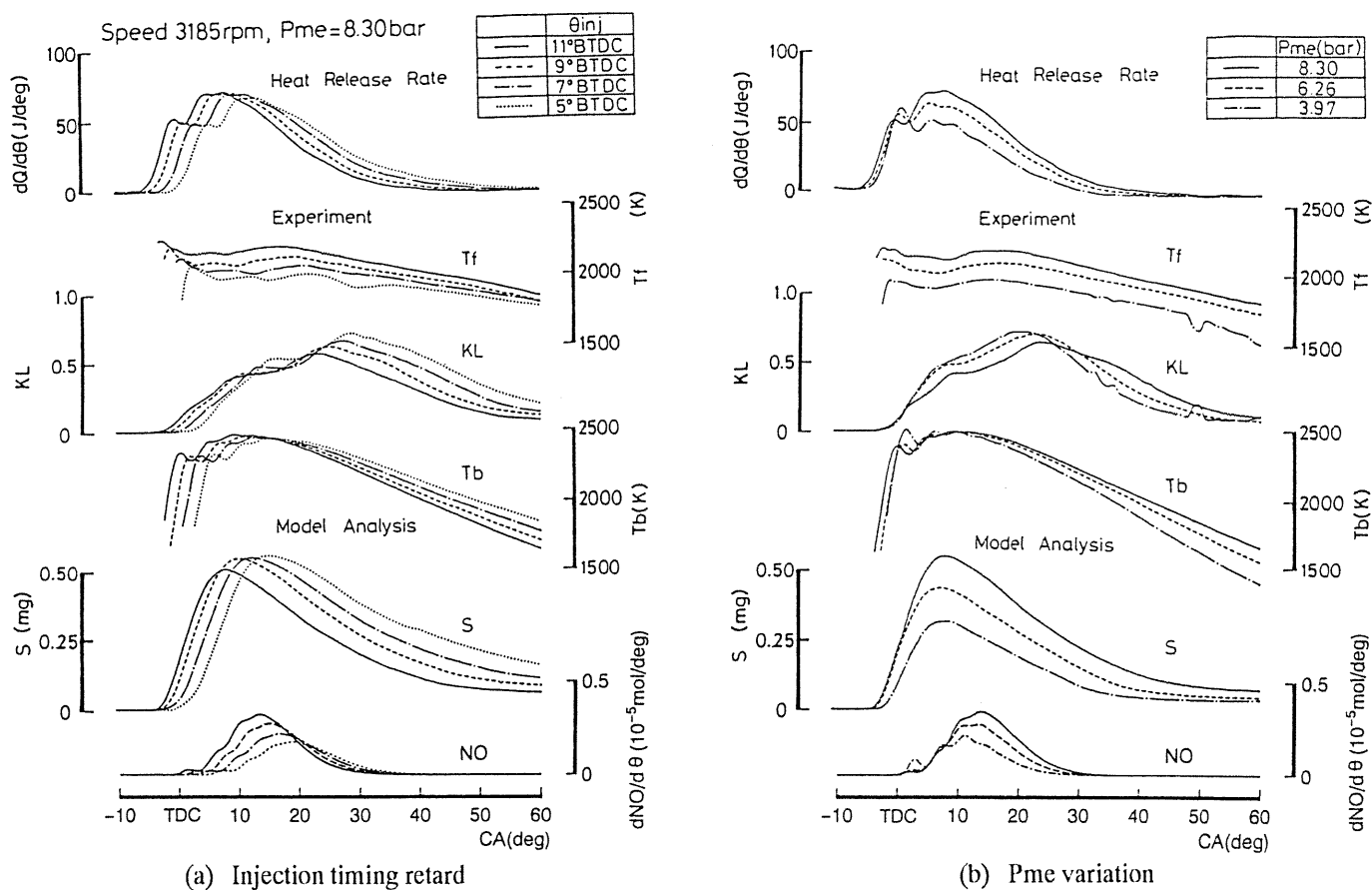


Fig.5 Comparison between experiment and analysis

COMPARISON BETWEEN EXPERIMENT AND ANALYSIS

Comparison of Gas Temperature and Soot Concentration

The calculated time histories of the burned gas temperature T_b and the net soot formation S are compared in Figs.5(a) and (b) with the experimental ones of the flame temperature T_f and the soot concentration parameter KL . In these figures, the experimental heat release rate is shown on the top and the calculated NO formation rate in the bottom. (a) shows the case of injection timing retard from 11 to 6 deg.BTDC and (b) shows the case of the brake mean effective pressure P_{me} variation. Comparing the temperatures T_f and T_b , it seems to be different apparently in both time histories because the maximum temperature position in crank angle differs from each other, however, the relative shifting of the maximum temperature position due to timing retard, the level of the maximum temperature during main combustion, and the temperature level at the end of combustion are nearly the same in both experiment and analysis. The experimental KL values have two peaks and its first peak position coincides well with the peak position of the calculated soot formation, however, there is no second peak in the analysis. The second highest peak in KL might be caused by the interaction between two adjacent fuel sprays due to the swirl flow. Generally speaking, the analytical results agree quantitatively or qualitatively with the experimental ones, except for the prediction of swirl effect.

Excess Air Ratio in the Burned Zone

The excess air ratio in the burned zone λ_{do} was estimated by the two-zone model analysis under various engine operation conditions, and compared in Fig.6 with the excess air ratio λ_f which is estimated from the model of a steady diffusion flame shown in Fig.7. This model is proposed in order to make clear the physical factor which dominates the excess air ratio λ_{do} , where the flame region consists of a steady fuel spray from a nozzle hole and a steady diffusion flame. In the cone-shaped flame region, l_1 is the fuel penetration length during ignition delay, and l_0 is the

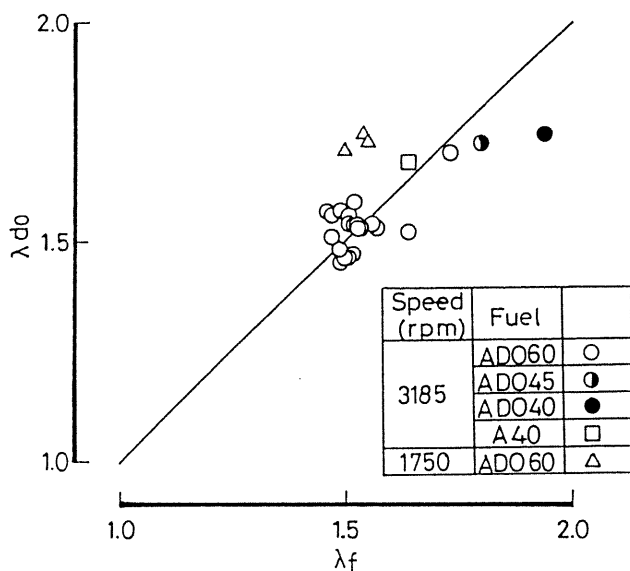


Fig.6 Correlation between two excess air ratios λ_{do} and λ_f

virtual penetration length with the mean excess air ratio of unity in the spray tip cross section. These values are estimated by the momentum theory derived by Wakuri et al.⁽⁶⁾ assuming that the straight cone could be maintained as shown in Fig.7 even though the cone shape should be strongly affected by the swirl and the spray impingement especially in the combustion chamber of a small-sized high speed diesel engine. And it is assumed that the whole cone is considered to be a quasi-flame region, the fuel burns in the hatched region of the cone under the theoretical mixture condition, and the burning rate is constant between the point B and C in Fig.7.

According to these assumptions, the excess air ratio λ_f is estimated by the equation of $\lambda_f = l_0 / (l_0 - l_1)$. Figure 6 shows the correlation between the burned zone excess air ratio λ_{do} determined by the two-zone model and the excess air ratio λ_f of the modeled diffusion flame. In spite of those rough assumptions, λ_{do} agrees well with λ_f and their variation is limited in a narrow range between 1.45 and 1.75. Nearly the same value is also shown in the literature⁽⁷⁾. On the other hand, there was little correlation between λ_{do} and the averaged excess air ratio in the cylinder. This means that the estimated excess air ratio in the burned zone λ_{do} is mainly dominated, as the first-order analysis, by the fuel spray characteristics and ignition delay. And it is noticed that the diffusion combustion excess air ratio λ_{do} does hardly vary by changing the fuel injection system such as injection timing or nozzle hole diameter, however, it varies by the fuel characteristics and the engine speed.

NOx REDUCTION FACTOR

The NOx reduction factor was analyzed in the experimental results by using the present two-zone model mainly on the point of view of the excess air ratio in the burned zone. Figures 8(a) and (b) show the analytical results of gas temperatures and NO formation rate under the constant excess air ratio condition $\lambda_{do} = 1.5$; (a) is the case of the timing retard and (b) is the case of the nozzle hole diameter reduction. The variation of NOx concentration in the exhaust gas is shown by solid lines in

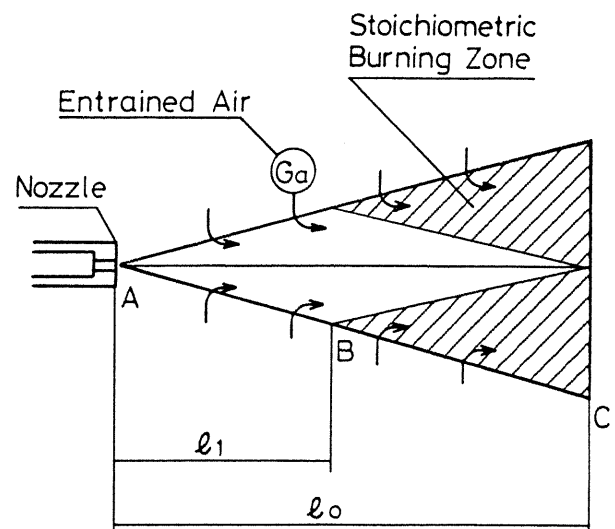


Fig.7 Steady diffusion flame model

Fig.9(a) and (b) respectively, where they are theoretically estimated by assuming the excess air ratio in the burned zone λ_d does not change by timing retard or by the reduction of nozzle hole diameter and also the time histories of combustion pressure

and heat release rate are the same for each parameter λ_d . In these figures, open circles indicate the calculated NO_x based on λ_f and solid circles show the measured one which results in λ_{d0} .

If λ_d would not change during timing retard from 11 to 4

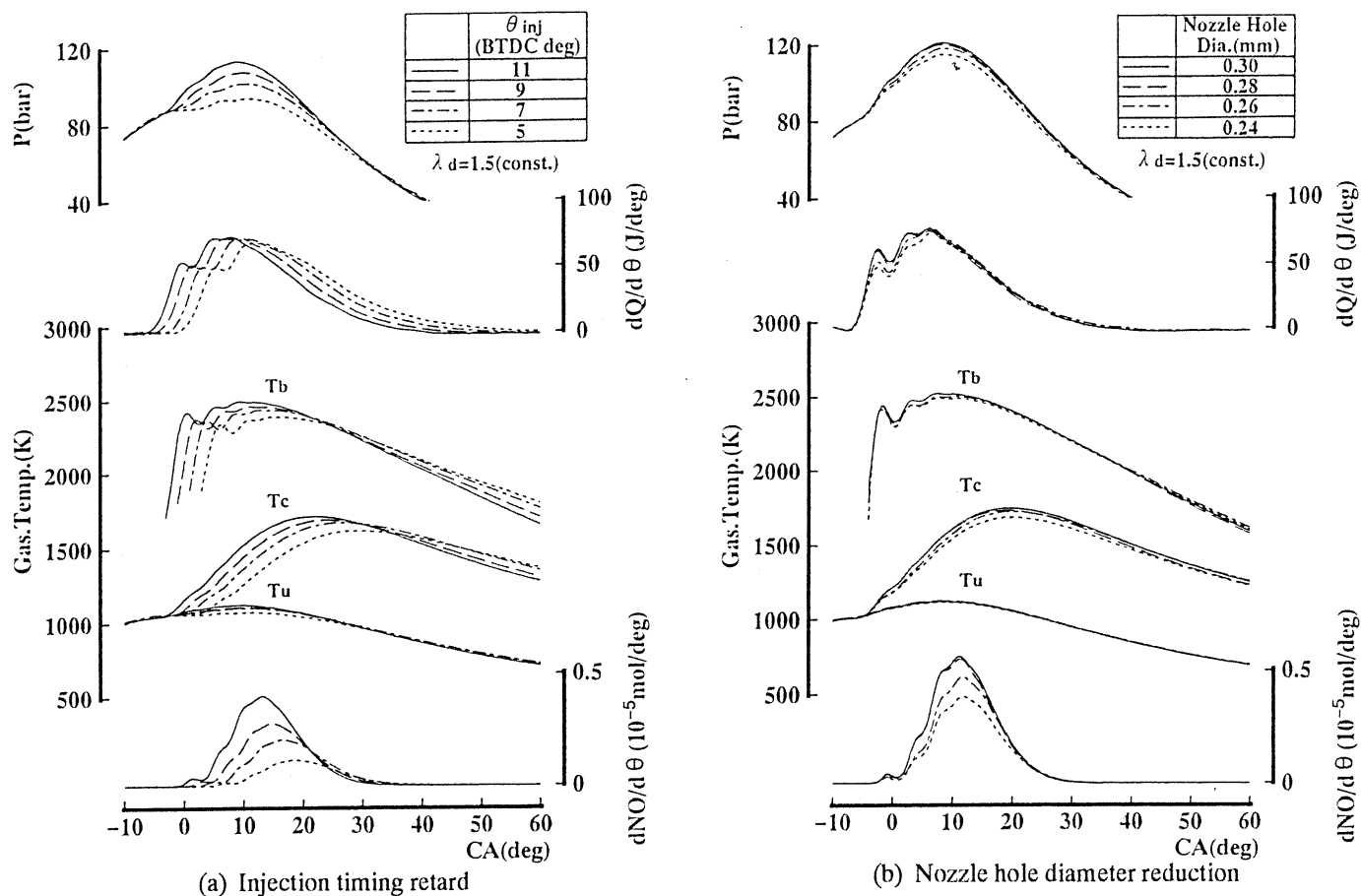


Fig.8 Analytical results of gas temperatures and NO formation rate

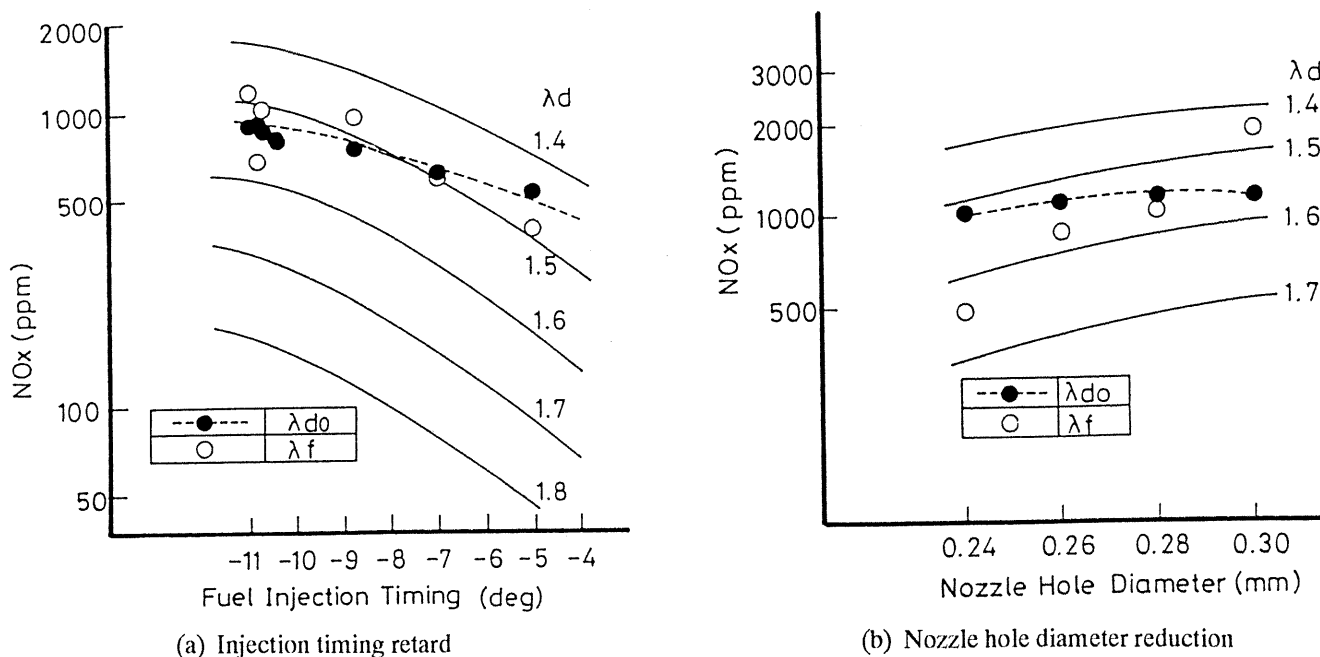


Fig.9 Calculated and experimental NO_x concentrations in the exhaust gas

Table 2 Summary of NOx reduction factor analysis

Physical Factor	Governing Factor	Practical Measures
Temperature	Gas Weight in Burned Zone	High Pressure Injection with Small Hole Nozzle
		Stratified F/W Injection Water Emulsified Fuel
	Specific Heat of Burned Gas	Water in Suction Air Exhaust Gas Recirculation
		Intercooling
Pressure	Mean Gas Temperature	Injection Timing Retard
		Pilot Injection Hole Dia. Reduction
		Ignition Improver
	Boost Pressure	Turbocharging

deg.BTDC, there could be a significant reduction in NOx, for example, it could be reduced from 1,200 to 300 ppm in the case of $\lambda_d = 1.5$. This is due to lowering the maximum temperature in the diffusion combustion period and, in addition, due to a large decrease in the maximum combustion pressure. On the other hand, the reduction due to timing retard in the measured NOx is less compared with the above calculated one because the excess air ratio in the burned zone decreased slightly at the retarded injection timing. A similar experimental result due to timing retard was shown in the literature⁽²⁾. Also in the case of nozzle hole reduction, a slight decrease in λ_{d0} is indicated by solid circles in Fig.7(b). As a result, a small amount of NOx was reduced by reducing the nozzle hole diameter despite that a large amount of NOx reduction was expected from a large increase in the excess air ratio as shown by open circles. This small reduction in NOx is due to small lowering of the maximum combustion pressure, because the smaller the nozzle hole, the less the injection rate is and the less the heat release rate is in the premixed combustion.

Table 2 shows summary of the analyzed NOx reduction factor. The fundamental physical factors which dominate NO formation are combustion temperature and combustion pressure. It was confirmed by the present two-zone model analysis that the NOx reduction due to timing retard is caused by decreases in both temperature and pressure through the variation of in-cylinder mean gas temperature, and the one due to nozzle hole reduction is caused by pressure variation. On the other hand, there are many practical measures proposed to reduce NOx, and they could be, or may be classified by the governing factors and by the physical factors in the manner as shown in Table 2 judging from the authors' present conception. It is difficult to classify clearly because pressure decrease due to timing retard affects the unburned gas temperature and finally results in a decrease in the burned gas temperature at the same time. It will be necessary more confirmation regarding the other measures except for injection timing retard and nozzle hole reduction. In the present analysis, only a small decrease in combustion temperature has a large reduction effect in NOx, as is well known, and also a significant reduction effect is confirmed in lowering the combustion pressure by timing retard and nozzle hole reduction.

CONCLUSIONS

Comparing the time histories of gas temperature and soot formation between the experiment and the analysis, the present two-zone model analysis showed its usefulness and effectiveness in evaluating the combustion process in a DI diesel engine, especially on the point of view of the excess air ratio in the burned zone. As a result, the following concluding remarks are obtained; (1) The excess air ratio of the burned zone is mainly dominated by the fuel spray characteristics and ignition delay and is hardly affected by the average excess air ratio in the cylinder. (2) A large NOx reduction due to timing retard is mainly caused by decreases of both the maximum combustion temperature and the maximum combustion pressure on the expansion stroke. (3) A small NOx reduction due to the reduced nozzle hole diameter is caused only by a decrease of combustion pressure based on a decrease of heat release rate in the premixed combustion.

ACKNOWLEDGEMENT

The authors would like to express their gratitude to Dr. F.Yoshizu, ZEXEL Co.Ltd. and Mr. T.Shimada, Mitsubishi Motor Corp. for their much support, and also to their laboratory's students in Nagasaki University for securing the experimental works.

REFERENCES

- (1) Ikegami, M., Shioji, M., and Koike, M., "A Stochastic Approach to Model the Combustion Process in Direct Injection Diesel Engine", Proc. of 20th Symposium (International) on Combustion / The Combustion Institute, pp.217-224 (1984)
- (2) Aoyagi, Y., Matsui, Y., Kamimoto, T., and Matsuoka, S., Trans. JSME, 47-413(B), pp.195-204 (1981), (in Japanese)
- (3) Hatakeyama, T., "Predicting Nitric Oxide Formation in Direct Injection Diesel Engine", Technical Report of Mitsubishi Heavy Industries, 12-3, pp.341-351 (1975), (in Japanese)
- (4) Morel, T., and Keribar, R., "Heat Radiation in D.I. Diesel Engine", SAE paper No.860445 (1986)
- (5) Hiroyasu, H., Arai, M., and Nishida, K., "Development and Use of Spray Combustion Modeling to Predict Diesel Engine Efficiency and Pollutant Emissions", Trans. JSME, 48-432(B) pp.1606-1622 (1982), also seen in Bulletin of JSME, 26-214, pp.569-583 (1983)
- (6) Wakuri, Y., Fujii, M., Amitani, T., and Tsuneya, R., "Studies on Penetration of Fuel Spray of Diesel Engine", Trans. JSME, 25-156, pp.820-826 (1959), also seen in Bulletin of JSME, 3-9, pp.123-130 (1960)
- (7) Sakane, A., Toshioka, S., Sumimoto, T., and Hamamoto, Y., "Effect of Fuel Injection Pressure on Diesel Combustion", Journal of M.E.S.J., 23-1, pp.47-54 (1988), (in Japanese)